Article

Inflammatory and alternatively activated macrophages independently induce metaplasia but cooperatively drive pancreatic precancerous lesion growth

Geou-Yarh Liou, Alicia K. Fleming Martinez, Heike R. Döppler, Ligia I. Bastea, Peter Storz

storz.peter@mayo.edu

Highlights
M1- and M2-polarized macrophages secrete factors that induce ADM

M1- and M2-secreted factors (SF) induce EGFR and TGFα in acinar cells to mediate ADM

Both M1 and M2 SF additively promote lesion growth via activation of MAP kinases

Figure360▷ For a Figure360 author presentation of this figure, see https://doi.org/10.1016/j.isci.2023.106820.

Article

Inflammatory and alternatively activated macrophages independently induce metaplasia but cooperatively drive pancreatic precancerous lesion growth

Geou-Yarh Liou,[1,2] Alicia K. Fleming Martinez,[1] Heike R. Döppler,[1] Ligia I. Bastea,[1] and Peter Storz[1,3,*]

SUMMARY

The innate immune system has a key role in pancreatic cancer initiation, but the specific contribution of different macrophage populations is still ill-defined. While inflammatory (M1) macrophages have been shown to drive acinar-to-ductal metaplasia (ADM), a cancer initiating event, alternatively activated (M2) macrophages have been attributed to lesion growth and fibrosis. Here, we determined cytokines and chemokines secreted by both macrophage subtypes. Then, we analyzed their role in ADM initiation and lesion growth, finding that while M1 secrete TNF, CCL5, and IL-6 to drive ADM, M2 induce this dedifferentiation process via CCL2, but the effects are not additive. This is because CCL2 induces ADM by generating ROS and upregulating EGFR signaling, thus using the same mechanism as cytokines from inflammatory macrophages. Therefore, while effects on ADM are not additive between macrophage polarization types, both act synergistically on the growth of low-grade lesions by activating different MAPK pathways.

INTRODUCTION

Human pancreatic ductal adenocarcinoma (PDA) is tightly associated with pancreatitis as a risk factor,[1] and numerous animal studies have shown that pancreatic inflammation can have a key role in the initiation of this cancer.[2,3] One effect of pancreatic inflammation is that it induces the dedifferentiation of acinar cells to a precursor cell-like phenotype with ductal features.[4] Cells that underwent such acinar-to-ductal metaplasia (ADM) can repopulate the pancreas after the inflammation is resolved.[5,6] However, if an oncogenic *Kras* mutation is present, ADM lesions progress to precancerous low-grade (LG) lesions with a fibrotic microenvironment.[4] In mice, different macrophage populations have been shown to be crucial to these processes.

Inflammatory (M1, IM) macrophages are chemoattracted by acinar cells carrying a *Kras* mutation[6] and produce factors such as CCL5/RANTES and tumor necrosis factor (TNF), which induce ADM in *ex vivo* culture.[7] Recent studies suggest that a common mechanism for different inducers of ADM is that they increase oxidative stress levels in acinar cells,[8] which drives PKD1-nuclear factor κ-B (NF-κB) signaling.[9] NF-κB, when active in acinar cells, induces the expression of epidermal growth factor receptor (EGFR) and its ligands TGFα and EGF[10]; and autocrine signaling through EGFR is the major driver of the ADM process.[11]

While inflammatory macrophages have roles in the initiation of ADM and lesion formation, the macrophage population surrounding established LG lesions increasingly includes alternatively activated (M2, AAM) macrophages.[12] LG lesion cells and DCLK1+ cells in these lesions produce IL-13, which is a driving factor mediating a polarization switch from an inflammatory to an alternatively activated macrophage phenotype.[12] In addition to this, in pancreatitis, pancreatic stellate cells have been shown to produce IL-4 and IL-13, also increasing the presence of alternatively activated macrophages.[13] In both studies, the IL-4/IL-13-initiated macrophage subpopulation has a key function as driver of the fibrotic lesion environment.[12–14]

In *in vivo* and *ex vivo* studies, this M2 macrophage population has been characterized by expression of *Chil3* (Ym1), *Arg1*, *Fizz1*, *Il1rn* (IL-1ra), *Il10* (IL-10), *Mrc1* (CD206), *C1qb*, and *Trem2* as markers,[12,15–18] and named the Ym1+ population. Ym1+ macrophages have been shown to promote lesion growth by producing TIMP1 and interleukin-1 receptor antagonist (IL-1ra),[12,18] and to activate quiescent pancreatic stellate cells and enhance fibrosis via TGFβ1.[18,19] Consequently, in animal studies, the depletion of this population

[1]Department of Cancer Biology, Mayo Clinic, Jacksonville, FL 32224, USA

[2]Department of Biological Sciences, Center for Cancer Research & Therapeutic Development, Clark Atlanta University, Atlanta, GA 30314, USA

[3]Lead contact

*Correspondence: storz.peter@mayo.edu

https://doi.org/10.1016/j.isci.2023.106820
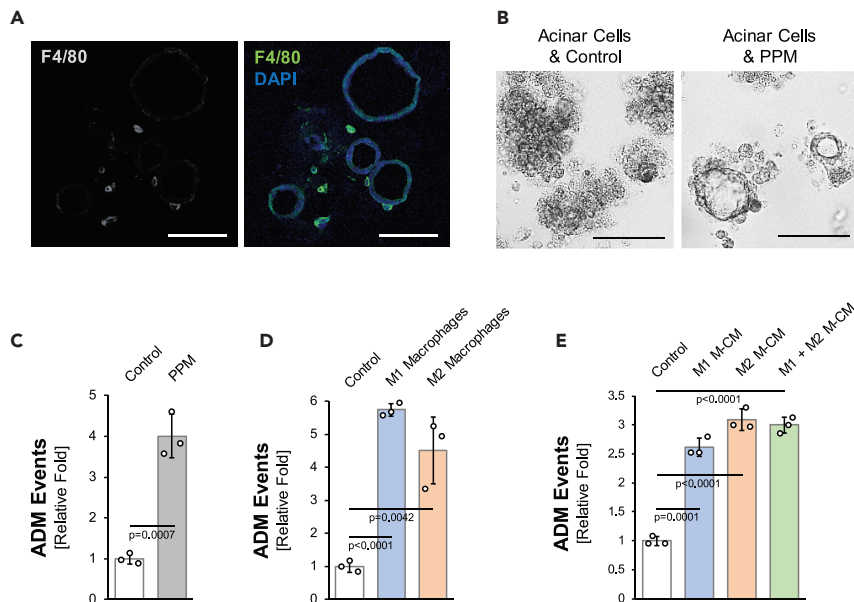
Figure 1. Both, inflammatory and alternatively activated macrophages induce acinar-to-ductal metaplasia (ADM)

(A) Non-transgenic (7-week-old) mice were treated with cerulein (75 μg/kg; hourly for 8 h, 2 days in a row) to induce acute pancreatitis. 24 h after the last injection, the pancreas was dissected and subjected to collagenase digestion. The pancreatic cell suspension was cultured in Matrigel overlayed with Waymouth complete media containing 10% FBS. At day 2, duct-like structures formed (ADM) and the sample was placed in a tissue cassette and processed as a tissue sample. Shown is a representative immunofluorescence staining for F4/80 (macrophages) and DAPI (to show ductal structures). Scale bars indicate 100 μm.

(B and C) Mouse primary pancreatic acinar cells and mouse primary peritoneal macrophages (PPM) were isolated and co-cultured in 3D explant culture. (B) shows representative pictures of the ductal structures formed at day 5 (scale bars indicate 200 μm), and (C) shows a quantification of ADM events (relative fold as compared to the control).

(D) Mouse primary pancreatic acinar cells were isolated and co-cultured in 3D explant culture with polarized mouse primary M1 or M2 macrophages. Ducts formed were quantified as described in the experimental procedures. Shown is the relative fold increase in ADM events as compared to the control treated samples.

(E) Mouse primary pancreatic acinar cells were isolated, seeded in 3D explant culture, and stimulated with conditioned media from polarized mouse primary M1 or M2 macrophages. Ducts formed were quantified as described in the experimental procedures. Shown is the relative fold increase in ADM events as compared to the control treated samples.
Experiments shown in C–E were performed in triplicates for at least 3 times and obtained similar results in each repeat. Statistical analysis between two groups was performed using the t-test. A p value of 0.05 was considered statistically significant and values are included in the graphs. Error bars represent the standard deviation.

by chemical means (treatment with pomalidomide) or by using IL-13 neutralization antibodies decreases not only numbers of LG lesions but also fibrosis surrounding lesions.[12,17,18]

The goal of the present study was to utilize explant and organoid culture to determine if induction of ADM and lesion growth strictly can be attributed to one macrophage polarization type or if there is an overlap in function between inflammatory and Ym1+ alternatively activated macrophages. Therefore, we determined and analyzed cytokines and chemokines secreted by these macrophages. We found that both polarization types independently induce acinar cell metaplasia, but signal additively to drive lesion growth.

RESULTS

Both, inflammatory and alternatively activated macrophages induce acinar-to-ductal metaplasia

We induced acute pancreatic inflammation in mice, isolated pancreatic cells, and embedded them in collagen 3D culture. After 2 days, acinar cell clusters transformed to typical duct-like structures (visualized with DAPI staining) with macrophages (F4/80 staining) either attached or in immediate proximity (Figure 1A). Using *ex vivo* organoid culture, we next investigated if these macrophages can drive the ADM process. We found that freshly isolated primary peritoneal macrophages (PPM) when co-cultured
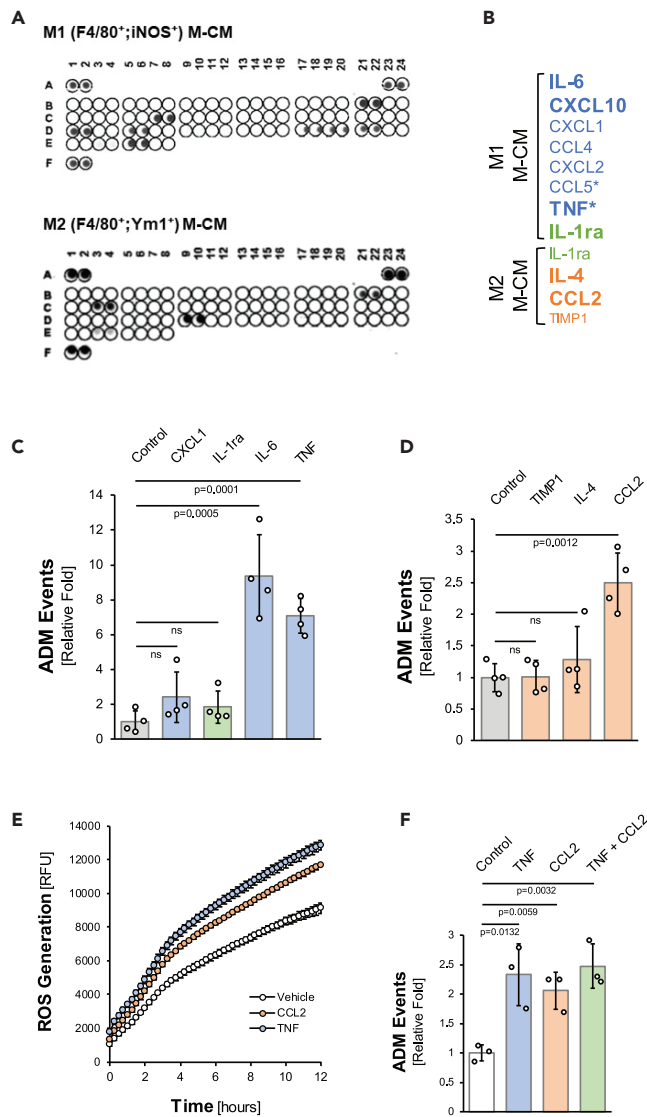
Figure 2. M1- and M2-derived factors can drive ADM independently

(A) Conditioned media from peritoneum-derived M1 (F4/80$^+$;iNOS$^+$) or M2 (F4/80$^+$;Ym1$^+$) were subjected to a mouse cytokine profiler array for detection of 40 different cytokines (see table in Figure S2A for cytokine identity and position on the array; A1/2, A23/24, and F1/2 contain positive controls). Experiments shown were performed in duplicates and obtained the same results in each repeat.

(B) List of cytokines/chemokines found in M1 macrophage-conditioned media (blue) and in M2 macrophage-conditioned media (orange) or in both (green). The bold font indicates high abundance, and smaller font size indicates weak abundance. The asterisk indicates previously identified factors that induce ADM.

(C and D) Mouse primary pancreatic acinar cells were isolated, seeded in 3D explant culture, and stimulated with vehicle (control), and 50 ng/mL CXCL1, IL-1ra, IL-6, TIMP1, IL-4, CCL2, or TNF (positive control). Ducts formed were quantified as described in the experimental procedures. Shown is the relative fold increase in ADM events as compared to the control treated samples. Error bars represent the standard deviation. Experiments shown were performed in triplicates for 3 times and each repeat obtained similar results. Statistical analysis between two groups was performed using a t-test. A p value of 0.05 was considered statistically significant and values are included in the graphs.

(E) Primary mouse pancreatic acinar cells were stimulated with CCL2 (50 ng/mL) or TNF (50 ng/mL) and labeled with H$_2$DFFDA. Generation of intracellular ROS (relative fluorescent units, RFU) was measured every 15 min over 12 h. For both cytokines, the increase in intracellular ROS was statistically significant with p < 0.0001 when determined at 4, 8 and 12 h, using a t-test and comparison of the cytokine treated samples to the control samples. Each point represents the mean at that time point and error bars represent the standard deviation.

Figure 2. *Continued*

(F) Primary mouse pancreatic acinar cells were isolated and seeded in 3D explant culture. Cells were treated with TNF (50 ng/mL), CCL2 (50 ng/mL) or both as indicated. Ducts formed were quantified as described in the experimental procedures. Shown is the relative fold increase in ADM events as compared to the control treated samples. Error bars represent the standard deviation. Experiments shown were performed in triplicates for at least 3 times and each repeat obtained similar results. Statistical analysis between two groups was performed using a t-test. A p value of 0.05 was considered statistically significant and values are included in the graphs.

with acinar cells can drive ADM (Figures 1B and 1C). To determine if this effect is due to a macrophage polarization type, we polarized PPM to M1 or M2 phenotypes (Figure S1A) before they were co-cultured with acinar cells. We found that both M1 and M2 macrophages can induce ADM at similar levels (Figure 1D). Eventually, to determine if direct contact between cell types is needed or if this event is driven by macrophage-secreted molecules, we compared conditioned media from both polarization types. Conditioned media from both M1 and M2 macrophages induced expression of ductal markers such as *Sox9* and *Muc1*,[20,21] and decreased expression of the acinar cell identity marker Mist1/*Bhlha1* (Figure S1B). Conditioned media of M1 and M2 macrophages induced ADM at similar levels (Figures 1E and S1C). Moreover, a combination of both CM was not additive, suggesting that both use a similar mechanism to induce ADM (Figure 1E).

M1-derived and M2-derived factors can drive ADM independently

Using cytokine arrays covering a set of 40 different cytokines and chemokines (Figure S2A), we next determined their expression pattern in CM from M1- and M2-polarized primary peritoneal macrophages. While both macrophage-conditioned media (M-CM) contained IL-1ra, presence of IL-6, CXCL10, CXCL1, CCL4, CXCL2, CCL5/RANTES, and TNF was specific to M1 M-CM, and presence of IL-4, CCL2, and TIMP1 specific to M2 M-CM (Figures 2A, 2B, and S2B). Of the factors only found in M1 M-CM, CCL5/RANTES and TNF previously were identified as inducers of ADM.[7] Of the remaining so far untested cytokines, we found IL-6, but not CXCL1 nor IL-1ra, capable of inducing ADM (Figure 2C). Of the M2 M-CM-secreted factors, we found that only CCL2 is a significant inducer of ADM (Figure 2D). Since TNF is one of the most prominent inducers of ADM in M1 M-CM, and CCL2 is the only inducer in our panel of cytokines that induces ADM in M2 M-CM, we used these two cytokines for further analyses.

We recently have shown that the increase in cellular oxidative stress levels is a common signaling feature for inducers of ADM, including TNF, CCL5,[8] and IL-6 (Figure S2C). We therefore tested if the M2-secreted molecule CCL2 also induces cellular oxidative stress. We found that CCL2 increased oxidative stress in acinar cells, similar to effects seen after TNF treatment (Figure 2E), suggesting that CCL2 triggers similar signaling events than other inducers of ADM. Both, M1-secreted TNF and M2-secreted CCL2 do not act additively or synergize with respect to driving ADM events (Figure 2F), supporting our previous observation in which we compared conditioned media from both macrophage subtypes (Figure 1E).

Macrophage-secreted factors induce ADM through upregulation of TGFα/EGFR signaling

A driving event of ADM downstream of oxidative stress is the upregulation of expression of EGFR and/or its ligands in acinar cells.[8,10,11,22–24] We therefore tested if both polarization types of macrophages can activate EGFR signaling in acinar cells. Both M1 M-CM and M2 M-CM (Figure 3A) upregulated the expression of *Egfr* and its ligand *Tgfa*, but not *Egf*, amphiregulin (*Areg*), or *Hbegf* (Figures S3A–S3C). Similarly, treatment with the M1- or M2-secreted ADM-inducing factors TNF and CCL2 led to an upregulation of *Egfr* and TGFα/*Tgfa* (Figure 3B). Moreover, combination of the EGFR inhibitor erlotinib with M1 M-CM and M2 M-CM (Figure 3C), or with TNF and CCL2 (Figure 3D) blocked ADM, confirming that ADM in all cases is driven through EGFR signaling.

Inflammatory and alternatively activated macrophages additively drive lesion growth through multiple factors

While both macrophage polarization types drive ADM through different chemokines but using the same mechanisms, we noted differences in the resulting ductal structures. In addition to ADM, M1 M-CM and M2 M-CM media each led to growth of ADM lesions as measured by a 1.8-fold and 1.6-fold increase in the average ductal area (Figures 4A and 4B). The combination of both showed an additive effect with an approximately 4.4-fold increase in the average ductal area (Figures 4A and 4B). This increase was neither due to TNF or CCL2 signaling nor a combination of both (Figure S4).
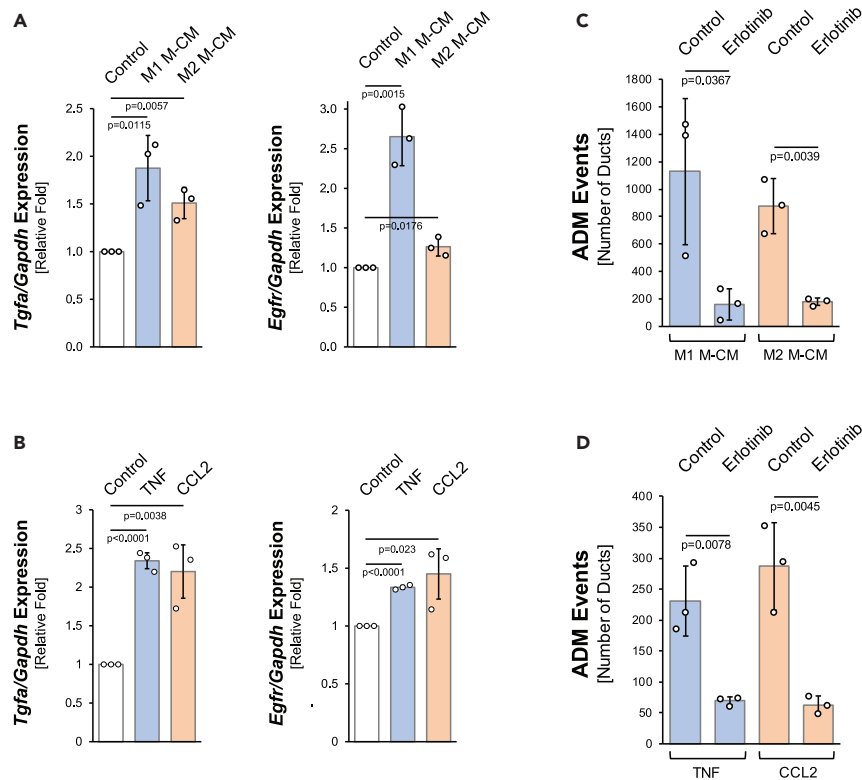
Figure 3. Macrophage-secreted factors induce ADM through upregulation of TGFα/EGFR signaling

(A and B) Mouse primary pancreatic acinar cells were isolated and stimulated with conditioned media from polarized mouse primary M1 or M2 macrophages (in A) or 50 ng/mL TNF or CCL2 (in B), as indicated. Expression of TGFα/*Tgfa* and *Egfr* mRNA was determined via qPCR and normalized to *Gapdh*. Shown is the relative fold change to the control. Error bars represent the standard deviation. Statistical analysis between two groups was performed using a t-test. A p value of 0.05 was considered statistically significant and values are included in the graphs. Experiments shown were performed in triplicates for 3 times and each repeat obtained similar results.

(C and D) Primary mouse pancreatic acinar cells were isolated and seeded in 3D explant culture. Cells were treated with erlotinib (500 nM) or control and stimulated with conditioned media from polarized mouse primary M1 or M2 macrophages (in C) or 50 ng/mL TNF or CCL2 (in D), as indicated. Ducts formed were quantified as described in the experimental procedures. Shown is the total number of ADM events/well. Error bars represent the standard deviation. Experiments shown were performed in triplicates for 3 times and each repeat obtained similar results. Statistical analysis between two groups was performed using a t-test. A p value of 0.05 was considered statistically significant and values are included in the graphs.

To further analyze effects of factors released from M1 or M2 macrophages on lesion growth, we used 3D organoid culture of primary PanIN lesion cells (described in the study by Fleming Martinez et al.[25]). Using this system, we previously had described IL-1ra as a factor that can drive lesion growth through activation of ERK1/2 signaling.[12] Our current data suggest that IL-1ra is present in supernatant from M1 and M2 macrophages, with M1 being the main producers (Figures 2A and 2B). However, the additive effects seen in Figure 4B suggest additional factors in M2 M-CM that drive lesion growth.

Of the factors that are only secreted by M2 macrophages, CCL2 and TIMP1 have been shown to moderately affect lesion growth through activating ERK1/2.[12,18] So far, no data are available on the effects of IL-4 on lesion growth, a factor that is also present in M2 M-CM (Figure 2A). The ductal area of lesions when treated with IL-1ra increased approximately 2-fold and with IL-4 1.5-fold. The combination of both, however, led to an approximately 5-fold increase (Figures 4C and 4D), indicating a synergistic effect similar to that seen for conditioned media from both macrophage populations. In summary, our data, using IL-4 as an example, show that M2 macrophages secrete multiple cytokines that can act additively to other M1- and M2-secreted factors such as IL-1ra to promote lesion growth.
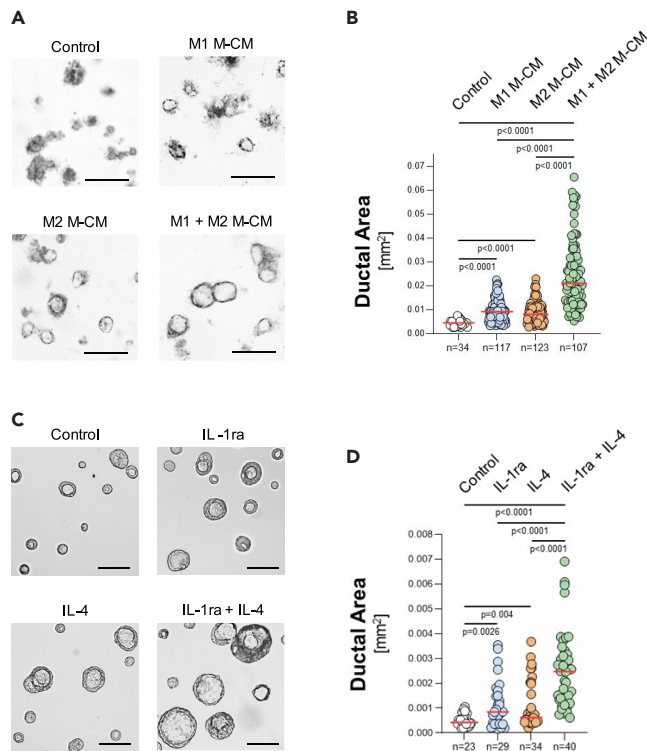
Figure 4. Inflammatory and alternatively activated macrophages additively drive lesion growth through multiple factors

(A and B) Mouse primary pancreatic acinar cells were isolated, seeded in 3D explant culture, and incubated with conditioned medium of M1- or M2-polarized mouse primary peritoneal macrophages as indicated. (A) Ductal structures formed by ADM events were documented. The bar indicates 500 μm. (B) Quantification of the ductal area of indicated numbers of ductal structures from each experimental condition shown in A. The red bar indicates the median. Statistical analysis between two groups was performed using a t-test. A p value of 0.05 was considered statistically significant and values are included in the figure.

(C and D) PanIN cells from KC mice were seeded in Matrigel culture and stimulated with control, IL-1ra (50 ng/mL), IL-4 (50 ng/mL) or both as indicated. (C) Ductal structures formed were documented at day 2. The bar indicates 100 μm (D) Quantification of the ductal area of indicated numbers of ductal structures from each experimental condition shown in C. The red bar indicates the median. Statistical analysis between two groups was performed using a t-test. A p value of 0.05 was considered statistically significant and values are included in the figure.

Synergistic effects of IL-1ra and IL-4 are due to activation of different proliferative MAPK pathways

ERK1/2 activity can be detected in mouse ADM and PanIN lesions *in vivo* and has been linked to lesion growth.[11,22] In 3D organoid assays, induction of lesion growth and activation of ERK1/2 is induced by IL-1ra.[12] However, the synergistic effects of IL-1ra combined with IL-4 suggest activation of additional proliferative signaling pathways. To test this, we focused on other mitogen-activated protein kinase (MAPK) pathways that are linked to proliferation such as activation of c-Jun N-terminal kinase ½ (JNK1/2) signaling. We found that while IL-1ra and IL-4 both activated p44-ERK at similar levels and were not acting additively (Figure 5A), IL-4 strongly activated JNK1/2 signaling (Figure 5B), suggesting that the observed synergistic signaling may be due to activation of additional MAPK pathways. Of note, the p38 MAPK signaling pathway was not activated by either of these cytokines (Figure S5A). As proof of principle, to test if ERK1/2 and JNK1/2 activation can occur in the same lesions *in vivo*, we stained serial sections of murine PanIN lesions from 24-week-old KC (p48[cre];LSL-Kras[G12D]) mice with phospho-T202/Y204-ERK1/2 and phospho-T183/Y185-JNK1/2 antibodies (Figure S5B). Our data suggest that both pathways are also active in LG lesions *in vivo*; however, a potential *in vivo* function for both MAPK pathways as drivers of lesion progression needs to be tested more rigorously in future studies.
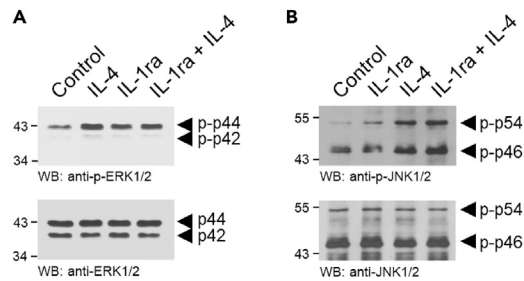
Figure 5. Synergistic effects of IL-1ra and IL-4 are due to activation of different proliferative MAPK pathways
(A and B) PanIN cells from KC mice were stimulated with control, IL-1ra (250 ng/mL), IL-4 (50 ng/mL) or both as indicated for 2 days. (A) Western blot analyses for ERK1/2 (p42/p44) and phospho-T202/Y204-ERK1/2 (p-p42 and p-p44); and (B) Western blot analyses for JNK1/2 (p46/p54) and phospho-T183/Y185-JNK1/2 (p-p46 and p-p54). Shown are representative figures from 3 independent experiments showing similar results in each repeat.

DISCUSSION

While a key role of the innate immune system in the initiation of pancreatic cancer is emerging, the contributions of different macrophage populations to this process are still ill-defined. Previous work suggested a model in which M1 drive the initiation of LG lesions,[7,12,26] while M2 drive lesion growth and fibrosis.[12,13,17,18] Our present study, suggesting that both macrophage polarization types can have redundant functions on ADM, but act synergistically to promote lesion growth, adds complexity to this model.

Pancreatic injury or inflammation (pancreatitis) is linked to macrophage infiltration into the pancreas.[27] Emerging evidence suggests that these macrophages do not originate from tissue-resident populations,[28] but rather are chemoattracted to the pancreas via factors such as ICAM1.[6] Pancreatitis in mice induces ADM, a dedifferentiation of acinar cells to a duct-like stage. After pancreatitis, ADM cells can mediate pancreatic regeneration,[5,14] but when oncogenic *Kras* mutations are present, ADM cells progress to precancerous LG lesions.[4,29] Pancreatitis-induced ADM was attributed to factors produced by inflammatory macrophages.[8,30]

Of the factors that can be detected in media from inflammatory (M1) macrophages (Figurse 2A and 2B), several have been shown to induce ADM. These include TNF, CCL5/RANTES,[7,8,26] and IL-6 (Figure 2C), while others such as CXCL10 and CXCL2[7] or CXCL1 and IL-1ra (both Figure 2C) do not affect ADM. In our present study, we now find that the supernatant of M2 macrophages also contains cytokines that induce ADM (Figures 1D and 1E), and further analysis indicates that CCL2 is a driving factor (Figure 2D). Moreover, we show that M1- or M2-induced ADM is not an additive effect (Figure 1E).

It recently was shown that the increase in cellular oxidative stress and reactive oxygen species (ROS)-driven activation of NF-κB and upregulation of EGFR signaling is a common underlying mechanism that drives ADM downstream of different inducers such as TNF, CCL5, and oncogenic KRAS.[8,10,11,22–24] We here show that IL-6 (Figure S2C) and CCL2 (Figure 2E) also increase cellular oxidative stress and thus may utilize the same signaling mechanisms. Of importance, M2-produced CCL2, like M1-produced TNF, upregulates the expression of EGFR and its ligand TGFα (Figure 3B). Moreover, M1- and M2-driven, as well as CCL2- and TNF-driven, ADM can be blocked with erlotinib (Figures 3C and 3D), further supporting that induction of EGFR signaling is the major driver of the ADM process downstream of these factors.

At this point, it is unclear if ROS, besides NF-κB,[8,10] also activates other transcription factors to drive ADM. Our data showing that IL-6 generates ROS (Figure S2C) and induces ADM (Figure 2C) may support this, since IL-6 can signal to both NF-κB[31] and signal transducer and activator of transcription 3 (STAT3).[32] Both NF-κB and STAT3 have been shown to induce ADM[4,7,10,33] but it is unclear how they cooperate in inducing EGFR signaling.

During pancreatitis or development of PDA, M1 undergo a polarization switch to M2.[12–14,17] This can be induced by IL-4 and IL-13 secreted from pancreatic stellate cells,[13] or by IL-13 secreted from PanIN lesion cells and DCLK1+ stem cells.[12] M2-produced factors then drive lesion growth (proliferation) via activation of ERK1/2.[12,18] Of these, IL-1ra, a factor that previously has been implicated in enhancing cell proliferation,[34] is most efficient, but this factor is produced by both M1 and M2 macrophages. Since our data indicated that

both M1 and M2 macrophages can act synergistically on lesion growth (Figure 4B), we tested if M2 macrophages activate additional MAPK pathways that have been previously involved in proliferation. By using the M2 macrophage-produced factor IL-4 (Figures 2A and the study by La Flamme et al.[35]) as an example, we show that M2 macrophages secrete cytokines that can act in synergism with M1/M2-secreted factors (such as IL-1ra) to promote lesion growth. This most likely is mediated via activation of JNK (Figures 5B and S5B), which previously had been linked to proliferative signaling during cancer development.[36]

While M1 and M2 macrophages both contribute to ADM and lesion growth, it should be noted that M2 have been shown to also express TGFβ.[37] At pancreatic LG lesions, M2 induce fibrosis,[12,17,18] EMT-like signaling, and a structure collapse in lesions via TGFβ1/SMAD4 signaling,[18] processes that are linked to the desmoplastic reaction and progression to high-grade lesions.

In summary, we used *ex vivo* organoid cultures to investigate the interplay between different subtypes of macrophages in pancreatic lesion formation and growth. We found that besides M1 macrophages, which have been described as inducers of ADM,[7] M2 macrophages also can initiate this transdifferentiation process. Moreover, both polarization types secrete factors that activate ERK1/2 and JNK1/2 MAPK to synergistically drive lesion growth (Graphical Abstract). Overall, this reveals aspects of PDA initiation and further highlights the importance of different macrophage populations in these processes.

LIMITATIONS

Our data reveal aspects of how different macrophage populations contribute to PDA initiation, but also need confirmation in future *in vivo* animal studies.

For example, we used *ex vivo* organoid cultures to investigate the interplay between different subtypes of macrophages in pancreatic lesion formation and growth. Our data revealed redundancy of M1 and M2 macrophages in inducing ADM, by engaging similar signaling mechanisms. *In vivo*, it is likely that M1 macrophages initiate the occurrence of ADM events, but that M2 macrophages once present can initiate the same signaling, thus increasing the number of pancreatic abnormal regions.

In our study, we also found that lesion growth is driven by both, M1- and M2-produced factors, which activate different proliferative MAPK signaling pathways. These findings may be exploited to develop new strategies to target the desmoplastic reaction, lesion growth, and progression. To develop these strategies, different combinations of MAPK inhibitors and targeting of M2 and/or M1 macrophages also need to be tested in future animal studies.

STAR★METHODS

Detailed methods are provided in the online version of this paper and include the following:

- KEY RESOURCES TABLE
- RESOURCE AVAILABILITY
  - Lead contact
  - Materials availability
  - Data and code availability
- EXPERIMENTAL MODEL AND SUBJECT DETAILS
  - Culture of primary cells
  - Mouse lines
- METHOD DETAILS
  - Antibodies and reagents
  - Primary pancreatic acinar cells: Isolation
  - PanIN organoids
  - Primary peritoneal macrophages: Isolation and polarization
  - Acinar-to-ductal metaplasia assays
  - Induction of acute pancreatitis in mice
  - Immunofluorescence (IF) and immunohistochemistry (IHC)
  - Cytokine arrays
  - RNA extraction and quantitative PCR
  - Western blotting

    ○ Measurement of ROS generation
  ● QUANTIFICATION AND STATISTICAL ANALYSES

AUTHOR CONTRIBUTIONS

Conceived and designed the experiments: A.K.F.M., H.R.D., L.I.B., G.Y.L., P.S. Performed the experiments: A.K.F.M., H.R.D., L.I.B., G.Y.L. Analyzed the data: G.Y.L., H.R.D., L.I.B., A.K.F.M., P.S. Wrote the paper: P.S., A.K.F.M.

DECLARATION OF INTERESTS

The authors declare no competing interests.

REFERENCES

1. Bansal, P., and Sonnenberg, A. (1995). Pancreatitis is a risk factor for pancreatic cancer. Gastroenterology 109, 247–251. https://doi.org/10.1016/0016-5085(95)90291-0.

2. Guerra, C., Collado, M., Navas, C., Schuhmacher, A.J., Hernández-Porras, I., Cañamero, M., Rodriguez-Justo, M., Serrano, M., and Barbacid, M. (2011). Pancreatitis-induced inflammation contributes to pancreatic cancer by inhibiting oncogene-induced senescence. Cancer Cell 19, 728–739. https://doi.org/10.1016/j.ccr.2011.05.011.

3. Guerra, C., Schuhmacher, A.J., Cañamero, M., Grippo, P.J., Verdaguer, L., Pérez-Gallego, L., Dubus, P., Sandgren, E.P., and Barbacid, M. (2007). Chronic pancreatitis is essential for induction of pancreatic ductal adenocarcinoma by K-Ras oncogenes in adult mice. Cancer Cell 11, 291–302. https://doi.org/10.1016/j.ccr.2007.01.012.

4. Storz, P. (2017). Acinar cell plasticity and development of pancreatic ductal adenocarcinoma. Nat. Rev. Gastroenterol. Hepatol. 14, 296–304. https://doi.org/10.1038/nrgastro.2017.12.

5. Criscimanna, A., Coudriet, G.M., Gittes, G.K., Piganelli, J.D., and Esni, F. (2014). Activated macrophages create lineage-specific microenvironments for pancreatic acinar- and beta-cell regeneration in mice. Gastroenterology 147, 1106–1118.e11. https://doi.org/10.1053/j.gastro.2014.08.008.

6. Liou, G.Y., Döppler, H., Necela, B., Edenfield, B., Zhang, L., Dawson, D.W., and Storz, P. (2015). Mutant KRAS-induced expression of ICAM-1 in pancreatic acinar cells causes attraction of macrophages to expedite the formation of precancerous lesions. Cancer Discov. 5, 52–63. https://doi.org/10.1158/2159-8290.CD-14-0474.

7. Liou, G.Y., Döppler, H., Necela, B., Krishna, M., Crawford, H.C., Raimondo, M., and Storz, P. (2013). Macrophage-secreted cytokines drive pancreatic acinar-to-ductal metaplasia through NF-kappaB and MMPs. J. Cell Biol. 202, 563–577. https://doi.org/10.1083/jcb.201301001.

8. Döppler, H.R., Liou, G.Y., and Storz, P. (2022). Generation of hydrogen peroxide and downstream protein kinase D1 signaling is a common feature of inducers of pancreatic acinar-to-ductal metaplasia. Antioxidants 11, 137. https://doi.org/10.3390/antiox11010137.

9. Storz, P., and Toker, A. (2003). Protein kinase D mediates a stress-induced NF-kappaB activation and survival pathway. EMBO J. 22, 109–120. https://doi.org/10.1093/emboj/cdg009.

10. Liou, G.Y., Döppler, H., DelGiorno, K.E., Zhang, L., Leitges, M., Crawford, H.C., Murphy, M.P., and Storz, P. (2016). Mutant KRas-induced mitochondrial oxidative stress in acinar cells upregulates EGFR signaling to drive formation of pancreatic precancerous lesions. Cell Rep. 14, 2325–2336. https://doi.org/10.1016/j.celrep.2016.02.029.

11. Ardito, C.M., Grüner, B.M., Takeuchi, K.K., Lubeseder-Martellato, C., Teichmann, N., Mazur, P.K., Delgiorno, K.E., Carpenter, E.S., Halbrook, C.J., Hall, J.C., et al. (2012). EGF receptor is required for KRAS-induced pancreatic tumorigenesis. Cancer Cell 22, 304–317. https://doi.org/10.1016/j.ccr.2012.07.024.

12. Liou, G.Y., Bastea, L., Fleming, A., Döppler, H., Edenfield, B.H., Dawson, D.W., Zhang, L., Bardeesy, N., and Storz, P. (2017). The presence of interleukin-13 at pancreatic ADM/PanIN lesions alters macrophage populations and mediates pancreatic tumorigenesis. Cell Rep. 19, 1322–1333. https://doi.org/10.1016/j.celrep.2017.04.052.

13. Xue, J., Sharma, V., Hsieh, M.H., Chawla, A., Murali, R., Pandol, S.J., and Habtezion, A. (2015). Alternatively activated macrophages promote pancreatic fibrosis in chronic pancreatitis. Nat. Commun. 6, 7158. https://doi.org/10.1038/ncomms8158.

14. Wu, J., Zhang, L., Shi, J., He, R., Yang, W., Habtezion, A., Niu, N., Lu, P., and Xue, J. (2020). Macrophage phenotypic switch

orchestrates the inflammation and repair/
regeneration following acute pancreatitis
injury. EBioMedicine 58, 102920. https://doi.
org/10.1016/j.ebiom.2020.102920.

15. Chen, Y., Kim, J., Yang, S., Wang, H., Wu, C.J.,
Sugimoto, H., LeBleu, V.S., and Kalluri, R.
(2021). Type I collagen deletion in
alphaSMA(+) myofibroblasts augments
immune suppression and accelerates
progression of pancreatic cancer. Cancer Cell
39, 548–565.e6. https://doi.org/10.1016/j.
ccell.2021.02.007.

16. Kemp, S.B., Steele, N.G., Carpenter, E.S.,
Donahue, K.L., Bushnell, G.G., Morris, A.H.,
The, S., Orbach, S.M., Sirihorachai, V.R.,
Nwosu, Z.C., et al. (2021). Pancreatic cancer is
marked by complement-high blood
monocytes and tumor-associated
macrophages. Life Sci. Alliance 4, e202000935.
https://doi.org/10.26508/lsa.202000935.

17. Bastea, L.I., Liou, G.Y., Pandey, V., Fleming,
A.K., von Roemeling, C.A., Doeppler, H., Li,
Z., Qiu, Y., Edenfield, B., Copland, J.A., et al.
(2019). Pomalidomide alters pancreatic
macrophage populations to generate an
immune-responsive environment at
precancerous and cancerous lesions. Cancer
Res. 79, 1535–1548. https://doi.org/10.1158/
0008-5472.CAN-18-1153.

18. Fleming Martinez, A.K., Döppler, H.R.,
Bastea, L.I., Edenfield, B.H., Liou, G.Y., and
Storz, P. (2022). Ym1(+) macrophages
orchestrate fibrosis, lesion growth, and
progression during development of murine
pancreatic cancer. iScience 25, 104327.
https://doi.org/10.1016/j.isci.2022.104327.

19. Apte, M., Pirola, R.C., and Wilson, J.S. (2015).
Pancreatic stellate cell: physiologic role, role
in fibrosis and cancer. Curr. Opin.
Gastroenterol. 31, 416–423. https://doi.org/
10.1097/MOG.0000000000000196.

20. Kopp, J.L., von Figura, G., Mayes, E., Liu, F.F.,
Dubois, C.L., Morris, J.P., 4th, Pan, F.C.,
Akiyama, H., Wright, C.V.E., Jensen, K., et al.
(2012). Identification of Sox9-dependent
acinar-to-ductal reprogramming as the
principal mechanism for initiation of
pancreatic ductal adenocarcinoma. Cancer
Cell 22, 737–750. https://doi.org/10.1016/j.
ccr.2012.10.025.

21. Strobel, O., Dor, Y., Alsina, J., Stirman, A.,
Lauwers, G., Trainor, A., Castillo, C.F.D.,
Warshaw, A.L., and Thayer, S.P. (2007). In vivo
lineage tracing defines the role of acinar-to-
ductal transdifferentiation in inflammatory
ductal metaplasia. Gastroenterology 133,
1999–2009. https://doi.org/10.1053/j.gastro.
2007.09.009.

22. Navas, C., Hernández-Porras, I.,
Schuhmacher, A.J., Sibilia, M., Guerra, C.,
and Barbacid, M. (2012). EGF receptor
signaling is essential for k-ras oncogene-
driven pancreatic ductal adenocarcinoma.
Cancer Cell 22, 318–330. https://doi.org/10.
1016/j.ccr.2012.08.001.

23. Means, A.L., Ray, K.C., Singh, A.B.,
Washington, M.K., Whitehead, R.H., Harris,
R.C., Jr., Wright, C.V.E., Coffey, R.J., Jr., and
Leach, S.D. (2003). Overexpression of
heparin-binding EGF-like growth factor in
mouse pancreas results in fibrosis and
epithelial metaplasia. Gastroenterology 124,
1020–1036. https://doi.org/10.1053/gast.
2003.50150.

24. Ray, K.C., Moss, M.E., Franklin, J.L., Weaver,
C.J., Higginbotham, J., Song, Y., Revetta,
F.L., Blaine, S.A., Bridges, L.R., Guess, K.E.,
et al. (2014). Heparin-binding epidermal
growth factor-like growth factor eliminates
constraints on activated Kras to promote
rapid onset of pancreatic neoplasia.
Oncogene 33, 823–831. https://doi.org/10.
1038/onc.2013.3.

25. Fleming Martinez, A.K., Döppler, H.R., Bastea,
L.I., Edenfield, B., Patel, T., Leitges, M., Liou,
G.Y., and Storz, P. (2021). Dysfunctional EGFR
and oxidative stress-induced PKD1 signaling
drive formation of DCLK1+ pancreatic stem
cells. iScience 24, 102019. https://doi.org/10.
1016/j.isci.2020.102019.

26. Deschênes-Simard, X., Mizukami, Y., and
Bardeesy, N. (2013). Macrophages in
pancreatic cancer: starting things off on the
wrong track. J. Cell Biol. 202, 403–405.
https://doi.org/10.1083/jcb.201307066.

27. Forsmark, C.E. (2013). Management of
chronic pancreatitis. Gastroenterology 144,
1282–1291.e3. https://doi.org/10.1053/j.
gastro.2013.02.008.

28. Pandey, V., Fleming-Martinez, A., Bastea, L.,
Doeppler, H.R., Eisenhauer, J., Le, T.,
Edenfield, B., and Storz, P. (2021). CXCL10/
CXCR3 signaling contributes to an
inflammatory microenvironment and its
blockade enhances progression of murine
pancreatic precancerous lesions. Elife 10,
e60646. https://doi.org/10.7554/eLife.60646.

29. Storz, P., and Crawford, H.C. (2020).
Carcinogenesis of pancreatic ductal
adenocarcinoma. Gastroenterology 158,
2072–2081. https://doi.org/10.1053/j.gastro.
2020.02.059.

30. Liou, G.Y., and Storz, P. (2015). Inflammatory
macrophages in pancreatic acinar cell
metaplasia and initiation of pancreatic
cancer. Oncoscience 2, 247–251. https://doi.
org/10.18632/oncoscience.151.

31. Wang, L., Walia, B., Evans, J., Gewirtz, A.T.,
Merlin, D., and Sitaraman, S.V. (2003). IL-6
induces NF-kappa B activation in the intestinal
epithelia. J. Immunol. 171, 3194–3201. https://
doi.org/10.4049/jimmunol.171.6.3194.

32. Lesina, M., Kurkowski, M.U., Ludes, K.,
Rose-John, S., Treiber, M., Klöppel, G.,
Yoshimura, A., Reindl, W., Sipos, B., Akira,
S., et al. (2011). Stat3/Socs3 activation by
IL-6 transsignaling promotes progression of
pancreatic intraepithelial neoplasia and
development of pancreatic cancer. Cancer
Cell 19, 456–469. https://doi.org/10.1016/j.
ccr.2011.03.009.

33. Miyatsuka, T., Kaneto, H., Shiraiwa, T.,
Matsuoka, T.A., Yamamoto, K., Kato, K.,
Nakamura, Y., Akira, S., Takeda, K., Kajimoto,
Y., et al. (2006). Persistent expression of
PDX-1 in the pancreas causes acinar-to-
ductal metaplasia through Stat3 activation.
Genes Dev. 20, 1435–1440. https://doi.org/
10.1101/gad.1412806.

34. Dewberry, R.M., King, A.R., Crossman, D.C.,
and Francis, S.E. (2008). Interleukin-1 receptor
antagonist (IL-1ra) modulates endothelial cell
proliferation. FEBS Lett. 582, 886–890.
https://doi.org/10.1016/j.febslet.2008.
02.021.

35. La Flamme, A.C., Kharkrang, M., Stone, S.,
Mirmoeini, S., Chuluundorj, D., and Kyle, R.
(2012). Type II-activated murine
macrophages produce IL-4. PLoS One 7,
e46989. https://doi.org/10.1371/journal.
pone.0046989.

36. Wagner, E.F., and Nebreda, A.R. (2009). Signal
integration by JNK and p38 MAPK pathways in
cancer development. Nat. Rev. Cancer 9,
537–549. https://doi.org/10.1038/nrc2694.

37. Rappolee, D.A., Mark, D., Banda, M.J., and
Werb, Z. (1988). Wound macrophages
express TGF-alpha and other growth factors
in vivo: analysis by mRNA phenotyping.
Science 241, 708–712. https://doi.org/10.
1126/science.3041594.

38. Means, A.L., Meszoely, I.M., Suzuki, K.,
Miyamoto, Y., Rustgi, A.K., Coffey, R.J.,
Jr., Wright, C.V.E., Stoffers, D.A., and
Leach, S.D. (2005). Pancreatic epithelial
plasticity mediated by acinar cell
transdifferentiation and generation of
nestin-positive intermediates.
Development 132, 3767–3776. https://doi.
org/10.1242/dev.01925.

39. Liou, G.Y., Döppler, H., Braun, U.B.,
Panayiotou, R., Scotti Buzhardt, M., Radisky,
D.C., Crawford, H.C., Fields, A.P., Murray,
N.R., Wang, Q.J., et al. (2015). Protein kinase
D1 drives pancreatic acinar cell
reprogramming and progression to
intraepithelial neoplasia. Nat. Commun. 6,
6200. https://doi.org/10.1038/ncomms7200.

40. Agbunag, C., Lee, K.E., Buontempo, S., and
Bar-Sagi, D. (2006). Pancreatic duct epithelial
cell isolation and cultivation in two-
dimensional and three-dimensional culture
systems. Methods Enzymol. 407, 703–710.
https://doi.org/10.1016/S0076-6879(05)
07055-2.

41. Zhang, X., Goncalves, R., and Mosser, D.M.
(2008). The isolation and characterization of
murine macrophages. Curr Protoc Immunol.
https://doi.org/10.1002/0471142735.
im1401s83.

42. Fleming Martinez, A.K., and Storz, P. (2019).
Mimicking and manipulating pancreatic
acinar-to-ductal metaplasia in 3-dimensional
cell culture. J. Vis. Exp. https://doi.org/10.
3791/59096.

STAR★METHODS

KEY RESOURCES TABLE

REAGENT or RESOURCE	SOURCE	IDENTIFIER
Antibodies		
Rabbit polyclonal anti-ERK1/2	Cell Signaling Technoloy	Cat# 9102; RRID:AB_330744
Rat monoclonal anti-F4/80	AbD Serotec/Bio-Rad	Cat# MCA497R; RRID:AB_323279
Rabbit polyclonal anti-iNOS	Abcam	Cat# ab3523; RRID:AB_303872
Rabbit polyclonal anti-JNK1/2	R&D Systems	Cat# AF1387; RRID:AB_2140743
Rabbit polyclonal anti-p38 MAPK	Cell Signaling Technology	Cat# 9212; RRID:AB_330713
Mouse monoclonal anti-phospho-T180/Y182-p38 MAPK	Cell Signaling Technology	Cat# 9216; RRID:AB_331296
Rabbit polyclonal anti-phospho-T183/Y185-JNK1/2	R&D Systems	Cat# AF1205; RRID:AB_2140857
Rabbit monoclonal anti-phospho-T202/Y204-ERK1/2	Cell Signaling Technology	Cat# 4370; RRID:AB_2315112
Rabbit polyclonal Ym1	STEMCELL Technologies	Cat# 60130; RRID:AB_2868482
Goat polyclonal anti-mouse IgG (HRP conjugated)	Jackson ImmunoResearch Labs	Cat# 115-035-003; RRID:AB_10015289
Goat polyclonal anti-rabbit IgG (HRP conjugated)	Jackson ImmunoResearch Labs	Cat#111-035-003; RRID:AB_2313567
Chemicals, peptides, and recombinant proteins		
4′,6-Diamidino-2-phenylindole dihydrochloride (DAPI)	Sigma-Aldrich	Cat# D8417
Cerulein	Sigma-Aldrich	Cat# C9026
Erlotinib	Selleckchem	Cat# S7786
Lipopolysaccharides (LPS) from *E. coli*	Sigma-Aldrich	Cat# L4391
Thioglycollate	BD Biosciences	Cat# 211716
Recombinant murine CCL2	PeproTech	Cat# 250-10
Recombinant murine CXCL1	PeproTech	Cat# 250-11
Recombinant murine EGF	PeproTech	Cat#315-09
Recombinant murine IFNγ	PeproTech	Cat# 315-05
Recombinant human IL-1ra	PeproTech	Cat# 200-01RA
Recombinant murine IL-4	PeproTech	Cat# 214-14
Recombinant murine IL-6	PeproTech	Cat# 216-16
Recombinant murine TIMP1	R&D Systems	Cat# 980-MT
Recombinant murine TNFα	PeproTech	Cat# 315-01A
Critical commercial assays		
BioRad Protein Assay	Bio-Rad	Cat# 5000006
Carboxy-H$_2$DFFDA ROS Assay	Invitrogen	Cat# C13293
High Capacity cDNA RT Kit	Applied Biosystems	Cat# 4368814
miRNeasy Mini Kit	Qiagen	Cat# 217004
Rneasy Plus Mini Kit	Qiagen	Cat# 74134
Proteome Profiler Mouse Cytokine Array Kit, Panel A	R&D Systems	Cat# ARY006
Taqman Fast Mix 2x	Applied Biosystems	Cat# 4352042
Experimental models: Cell lines		
Mouse: Primary pancreatic acinar cells	Method[6,8,25,38]	N/A
Mouse: Primary PanIN organoids	Method[12,40]	N/A
Mouse: Primary peritoneal macrophages	Method[17,28,41]	N/A
Experimental models: Organisms/strains		
Mouse: Ptf1a/p48cre/+ and LSL-KrasG12D/+ mouse strains	Mayo Clinic[6]	N/A
Mouse: non-transgenic mice with B6/129 background	Mayo Clinic	N/A

Continued

REAGENT or RESOURCE	SOURCE	IDENTIFIER
Oligonucleotides		
qPCR primer/probe: *Gapdh*	ThermoFisher Scientific	Mm99999915_g1
qPCR primer/probe: *Egf*/EGF	ThermoFisher Scientific	Mm00438696_m1
qPCR primer/probe: *Egfr*/EGFR	ThermoFisher Scientific	Mm01187858_m1
qPCR primer/probe: *Tgfa*/TGFa	ThermoFisher Scientific	Mm00446232_m1
qPCR primer/probe: *Areg*/AREG	ThermoFisher Scientific	Mm01354339_m1
qPCR primer/probe: *Hbegf*/HB-EGF	ThermoFisher Scientific	Mm00439306_m1
qPCR primer/probe: *Sox9*	ThermoFisher Scientific	Mm00448840_m1
qPCR primer/probe: *Muc1*	ThermoFisher Scientific	Mm00449604_m1
qPCR primer/probe: *Bhlha15*/Mist1	ThermoFisher Scientific	Mm00627532_s1
Software and algorithms		
Aperio ImageScope v12.4.3	Leica Biosystems	RRID:SCR_020993
BioRender	BioRender	RRID:SCR_018361
GraphPad Prism v9.2.0	GraphPad Sofware	RRID: SCR_002798
Image J	https://imagej.nih.gov/ij/	RRID:SCR_003070
Other		
Aperio AT2 Digital Scanner	Leica Biosystems	RRID:SCR_021256
Aperio FL Slide Scanner	Leica Biosystems	RRID:SCR_022191
BioTek Synergy HT plate reader	BioTek	RRID: SCR_020536
Quantstudio 7 Flex Real-Time PCR System	Applied Biosystems	RRID: SCR_020245
Bovine Pituitary Extract	Gibco/Thermo Scientific	Cat# 13028014
Cholera Toxin	Sigma-Aldrich	Cat# C8052
Collagen I, rat tail	Corning	Cat# 354236
Collagen I, bovine	R&D Systems	Cat# 3442-050-01
Collagenase I	Millipore/Sigma	Cat# C0130
D-glucose	Sigma-Aldrich	Cat# G8270
Dexamethasone	Sigma-Aldrich	Cat# D1756
Fetal Bovine Serum (FBS)	Gemini	Cat# 100-106
Insulin-transferrin-selenium (ITS)+ pre-mix	Corning	Cat# 354352
Matrigel	Corning Inc.	Cat# 354234
Nicotinamide	Sigma-Aldrich	Cat# N3376
Penicillin/streptomycin	Gibco/Thermo Scientific	Cat# 15140-122
RPMI-1640	Lonza	Cat# 12-115F
Soybean trypsin inhibitor type I	AMRESCO	Cat# K213
Triiodo-L-thyronine	Sigma-Aldrich	Cat# T6397
Waymouth MB 752/1 Medium	Sigma-Aldrish	Cat# W1625-10X1L

RESOURCE AVAILABILITY

Lead contact

Further information and requests for resources and reagents should be directed to and will be fulfilled by the lead contact, Peter Storz (storz.peter@mayo.edu).

Materials availability

This study did not generate any new unique reagents.

Data and code availability

- Data reported in this paper will be shared by the lead contact upon request.

- This paper does not report original code.

- Any additional information required to reanalyze the data reported in this paper is available from the lead contact upon request.

EXPERIMENTAL MODEL AND SUBJECT DETAILS

Culture of primary cells

All cells were cultured at 37 °C with 5% CO_2. Primary pancreatic acinar cells from mice were cultured in Waymouth Complete Media (Waymouth MB 752/1 Medium with 1% FBS, 0.1 mg/ml trypsin inhibitor, and 1 μg/ml dexamethasone). Culture media for primary PanIN organoids consisted of DMEM/F12 media (Sigma-Aldrich) containing 5% FBS, 25 μg/ml bovine pituitary extract (Gibco/Thermo Scientific, Waltham, MA), 20 ng/ml EGF, 0.1 mg/ml soybean trypsin inhibitor type I (AMRESCO, Solon, OH), 5 mg/ml D-glucose (Sigma-Aldrich), 1.22 mg/ml nicotinamide (Sigma-Aldrich), 5 nM *triiodo-L-thyronine* (Sigma-Aldrich), 1 μM dexamethasone (Sigma-Aldrich), 100 ng/ml cholera toxin (Sigma-Aldrich), 5 ml/l insulin-transferrin-selenium (Corning) and 100 U/ml penicillin/streptomycin (Gibco/Thermo Scientific). Primary peritoneal macrophages were cultured in RPMI-1640 containing 10% FBS and 1% Pen/Strep. Male and female mice were used in approximately equal numbers for all primary cell isolations.

Mouse lines

Male and female mice were randomly assigned to treatment groups. The ages of the mice are noted for each experiment in the method details. Ptf1a/p48cre/+ and LSL-KrasG12D/+ mouse strains, as well as genotyping have been described previously.[6] All animal experiments were performed in accordance with relevant institutional and national guidelines and regulations and were approved by the Mayo Clinic IACUC committee.

METHOD DETAILS

Antibodies and reagents

All antibodies and reagents are identified in the key resources table. Additional information on dilution of all antibodies used for immunohistochemistry, immunofluorescence, and Western blotting are provided in Table S1.

Primary pancreatic acinar cells: Isolation

The protocol for isolation of murine primary pancreatic acinar cells was described in detail before.[8,25,38,39] In brief, the pancreas of C57BL/6J mice was washed twice with HBSS media (4 °C), minced into 1 to 5 mm pieces and digested with collagenase I (37 °C, shaker). The digestion was terminated by addition of an equal volume of HBSS media (4 °C) with 5% FBS. The pieces were washed twice (HBSS plus 5% FBS) and pipetted through 500 μm and 105 μm meshes, and the resulting acinar cell suspension was added dropwise to 20 ml HBSS plus 30% FBS. Acinar cells were pelleted (1000 rpm, 2 min, 4°C) and re-suspended in 10 ml Waymouth complete media.

PanIN organoids

PanIN organoids (previously described in[12,40] were generated by seeding primary duct-like cells isolated from pancreata of 6-week-old Pdx1[Cre/+];Kras[G12D/+] mice in PanIN organoid media. For organoid culture, single cells were seeded on top of Matrigel (200 μl/well of a 24 well plate) and then stimulated as indicated. The area of ductal structures formed was determined using Image J software.

Primary peritoneal macrophages: Isolation and polarization

Non-transgenic mice at 10-20 weeks of age were injected with 2 ml of 5% aged thioglycollate. After five days, mice were euthanized and primary peritoneal macrophages (PPM) were collected by washing the peritoneal cavity with cold media (RPMI-1640 + 10% FBS + 1% Penicillin Streptomycin), as described in detail before.[18,28,41] Isolated PPM were plated onto 10 cm dishes, and once completely adhered, washed 3 times to remove non-adherent cells, before fresh media was added. Further polarization to IM and AAM was obtained by stimulation with 10 ng/ml LPS and 20 ng/ml murine IFN gamma (for IM polarization), or

with 20 ng/ml murine IL-4 (for AAM polarization), for 24 hours. After polarization, macrophages (on plate) were washed in macrophage media before experiments were conducted.

Acinar-to-ductal metaplasia assays

This method is described in detail in ref.[42] In short, cell culture plates were coated with collagen I/Waymouth media (w/o supplements) and freshly isolated primary pancreatic acinar cells were added. The cell/gel mixture was overlayed with Waymouth complete media, which was replaced every other day. Inhibitors or compounds were added at indicated concentrations. If not indicated otherwise in the figure legend, numbers of ducts per well were counted at day 5, and photos were taken to document cellular structures.

Induction of acute pancreatitis in mice

To induce acute pancreatitis in mice, cerulein (75 μg/kg) was injected intraperitoneally (IP) hourly for 8 hours, for two days in a row. 24 hours after the last injection the pancreas was dissected and further processed. All animal experiments were performed in accordance with institutional and national guidelines and regulations and were approved by the Mayo Clinic IACUC committee.

Immunofluorescence (IF) and immunohistochemistry (IHC)

For immunofluorescence, samples were washed in PBS, fixed in 4% paraformaldehyde in PBS (15 min, 37 °C), washed again in PBS, permeabilized using 0.1% Triton X-100 in PBS (2 min, RT) and then incubated with 100 mM glycine in PBS (2 min, RT). After blocking with 3% BSA, 0.05% Tween in PBS (30 min, RT) samples were incubated with primary antibodies (listed in Table S1) overnight at 4 °C. Samples then were washed in PBS, incubated with Alexa Fluor secondary antibodies (1:800; Invitrogen, Waltham, MA) and DAPI (0.25 μg/ml), as indicated, for 2 hours at RT, and washed in PBS. Fluorescent and brightfield images were taken using an Olympus IX71 (Olympus Scientific Solutions, Shinjuku City, Tokyo, Japan).

For immunohistochemistry, slides were deparaffinized and rehydrated and antigen retrieval and blocking were performed as previously described in detail.[25] For DAB immunohistochemistry, primary antibodies (as listed in Table S1) were diluted in Antibody Diluent Background Reducing Solution (DAKO) and visualized with the EnVision Plus Anti-Rabbit Labelled Polymer Kit (DAKO). For fluorescent immunohistochemistry (IF-IHC), slides were incubated with indicated primary antibodies (listed in Table S1) in Antibody Diluent Background Reducing solution at 4 °C overnight. After 3 washes with 0.05% Tween-20/PBS, Alexa Fluor 488, 568, or 647 labeled secondary antibodies (Invitrogen) were added (1:500, RT) for 1 hour with DAPI (0.5 μg/ml). LabVision PermaFluor (Thermo Scientific) was used as mounting medium. Images were captured using the Aperio AT2 Digital Scanner and Aperio FL Slide Scanner (Leica Biosystems, Wetzler, Germany) with ImageScope software.

Cytokine arrays

Indicated cells were starved for 48 hours and supernatants were analyzed for a panel of 40 cytokines using a mouse cytokine array (Proteome Profiler Mouse Cytokine Array Kit Panel A; R&D Systems).

RNA extraction and quantitative PCR

RNA extraction was performed using the RNeasy Plus Mini Kit (Qiagen, Hilden, Germany) and miRNeasy Mini Kit (Qiagen, Hilden, Germany), and cDNA was prepared using the High-Capacity cDNA RT Kit (Applied Biosystems, Waltham, MA). TaqMan Fast Mix 2x (Applied Biosystems) was used to prepare qPCR reactions with the TaqMan primer/probe sets noted in the key resources table. Samples were run on a QuantStudio 7 Flex Real-Time PCR System (Applied Biosystems). For analyses all C_T values were normalized to *Gapdh* and fold changes were calculated using the $\Delta\Delta C_T$ method.

Western blotting

For Western blotting, cells were washed three times with PBS (140 mM NaCl, 2.7 mM KCl, 8 mM Na2HPO4, 1.5 mM KH2PO4, pH 7.2; ice-cold) and lysed with Lysis Buffer A (50 mM Tris-HCl, pH 7.4, 1% Triton X-100, 150 mM NaCl, 5 mM EDTA, pH 7.4) plus protease inhibitor cocktail (Sigma-Aldrich, St. Louis, MO). After a 30 min incubation on ice lysates were centrifuged (13,000 rpm, 4 °C, 15 minutes), supernatants collected and the protein concentration measured using the BioRad Protein Assay (BioRad, Hercules, CA). After addition of 2x Laemmli buffer, samples were subjected to SDS-PAGE, transferred to nitrocellulose

membrane, and proteins of interest were detected using indicated specific antibodies and HRP-conjugated secondary antibodies at dilutions indicated in Table S1.

Measurement of ROS generation

Primary pancreatic acinar cells were isolated and stimulated as indicated. Cells were collected, centrifuged (233 xg, 2 min), resuspended in phenol red-free (PRF) HBSS, labeled with H_2DFFDA (20 μM, 45 min, 37 °C, 5% CO_2), washed two times (233 xg, 2 min) in PRF HBSS before being resuspended in PRF Waymouth complete media (0.1 mg/ml Soybean Trypsin Inhibitor, 1 μg/ml Dexamethasone, 500 μl FBS in 50 ml Waymouth MB 752/1). ROS generation over indicated time was determined using a BioTek Synergy HT plate reader (BioTek, Winooski, VT) at Ex 485/20/Em 528/20 and gain 55.

QUANTIFICATION AND STATISTICAL ANALYSES

All cell biological and biochemical experiments have been performed independently of each other at least 3 times. For ADM assays, biological replicates were done using pancreata from different mice. Quantification of ductal areas was performed using ImageJ. Data, when presented as bar graphs, show individual values (dots), mean and ± SD. If not stated otherwise in the figure legends, p values were acquired with the unpaired student's *t*-test with Welch's correction or ANOVA when more than two groups were compared to each other, using GraphPad software (GraphPad Inc., La Jolla, CA). The p values (when significant) are included in the graphs, and $p < 0.05$ was considered statistically significant.